

Relationship of ^{82}Rb PET territorial myocardial asynchrony to arterial stenosis

Andrew Van Tosh, MD,^a John R. Votaw, PhD,^b C. David Cooke, MSSE,^b
J. Jane Cao, MD,^a Christopher J. Palestro, MD,^{c,d} and Kenneth J. Nichols, PhD^{c,d}

^a Research Department, St. Francis Hospital, Roslyn, NY

^b Emory University, Atlanta, GA

^c Department of Radiology, Donald and Barbara Zucker School of Medicine at Hofstra/
Northwell, Hempstead, NY

^d Northwell Health, New Hyde Park, NY

Received Mar 21, 2018; accepted Jun 6, 2018

doi:10.1007/s12350-018-1350-4

Objective. ^{82}Rb PET/CT rest/regadenoson-stress data enable quantification of left ventricular rest and stress function, perfusion, and asynchrony. Our study was conducted to determine which parameters best identify patients with multi-vessel disease (MVD) and individual stenosed arteries.

Methods. PET/CT data were reviewed retrospectively for 105 patients referred for evaluation of CAD, who also underwent angiography. % arterial stenosis was determined quantitatively at a core laboratory. Severe stenosis was defined as $\geq 70\%$, and MVD as 2 or more stenosed arteries. Segmental MBF was calculated from first-pass data for arterial territories. Regional rest and stress systolic and diastolic asynchrony (Asynch) scores were determined from visual examination of phase polar maps.

Results. 65 vessels had stenoses $\geq 70\%$. 15 patients had MVD. ROC area under curve (ROC AUC) for identifying patients with MVD was 83% for Asynch and 73% for MFR. ROC AUC for identifying individual arterial territories with stenoses $\geq 70\%$ was 81% and 72% for Asynch and MFR.

Conclusion. ^{82}Rb PET/CT accurately identified patients with MVD and individual stenosed territories, with regional asynchrony measurements contributing significantly to identify patients with CAD. (J Nucl Cardiol 2020;27:575–88.)

Key Words: ^{82}Rb • PET • myocardial perfusion • asynchrony • angiography

Electronic supplementary material The online version of this article (<https://doi.org/10.1007/s12350-018-1350-4>) contains supplementary material, which is available to authorized users.

The authors of this article have provided a PowerPoint file, available for download at SpringerLink, which summarises the contents of the paper and is free for re-use at meetings and presentations. Search for the article DOI on SpringerLink.com.

Funding This investigation was supported in part by grants from Astellas Pharma Global Development Inc. to St. Francis Hospital and R01HL094438 and R44HL123069 to Emory University. John R.

Votaw, C. David Cooke and Kenneth J. Nichols participate in royalties from Syntermed, Inc.

Reprint requests: Kenneth J. Nichols, PhD, Department of Radiology, Donald and Barbara Zucker School of Medicine at Hofstra/Northwell, Hempstead, NY; knichols@northwell.edu

1071-3581/\$34.00

Copyright © 2018 American Society of Nuclear Cardiology.

Abbreviations

Asynch	Asynchrony measure
EF	Ejection fraction
LAD	Left anterior descending
LCX	Left circumflex
LV	Left ventricle
MBF	Myocardial blood flow
MFR	Myocardial flow reserve
MVD	Multi-vessel disease
RCA	Right coronary artery
ROC AUC	Receiver operating characteristics area under curve

See related editorial, pp. 581–591

INTRODUCTION

Cardiac positron emission tomography (PET) is an accurate method of diagnosing coronary artery disease (CAD). Using qualitative analysis and/or semi-quantitative relative regional uptake scores, PET achieves higher sensitivity, specificity, and accuracy for CAD than SPECT.^{1,2} This has been attributed to PET's use of high energy annihilation photons, higher spatial resolution, and validated attenuation correction. PET may be an underutilized nuclear technique, particularly in patients with an increased likelihood of false positive or equivocal SPECT results.³

When dynamic PET data are analyzed by kinetic models of tracer uptake, absolute values of rest and stress myocardial blood flow (MBF) can be measured, provided that corrections are applied for partial volume effects, count spillover, arterial tracer input, and extraction fraction.^{4,5} Animal experiments have validated PET measurements against MBF determined by microspheres for several PET tracers, including ⁸²Rb.⁶ Quantification of MBF has been shown to improve diagnosis of CAD,⁷ effectively ruling out functionally severe CAD when MBF is above threshold levels.⁸ MBF also aids in predicting major adverse cardiac events, particularly in patients with normal or near-normal relative perfusion.^{9,10} Based on studies such as those cited above, and on over 40 other studies of in excess of 5,400 patients,¹¹ quantification of myocardial blood flow with PET has now been approved for reimbursement by CMMS as of January 1, 2018.¹²

An important question at this juncture is whether MBF and myocardial flow reserve (MFR) are the best parameters for diagnosing CAD. In previous studies, MFR algorithms were often used in select patient groups, with exclusions for prior CABG and angioplasty,¹³ although some studies evaluated less restricted populations.¹⁴ Techniques to quantify MFR by PET are

now more widespread; therefore it is important to determine its value in unselected patients. While many prior studies evaluating PET MFR accuracy for diagnosing CAD used qualitatively interpreted coronary angiograms as the reference standard, it is important to recognize that even expert qualitative interpretations of coronary angiograms may vary considerably.¹⁵ Comparing PET MFR determinations to quantitative coronary angiography would therefore be desirable.

In this retrospective investigation we evaluated accuracy of PET for detecting CAD with quantitation of MFR in an unselected population of patients, including those with MI, previous CABG and PCI. MFR was evaluated along with other parameters vs quantitative coronary angiography as the reference standard. We sought to determine how this technology might best be used to detect CAD.

MATERIALS AND METHODS

Patients

Data were analyzed retrospectively for 105 patients (age 69 ± 13 years; 42 females; 63 males) with known or suspected CAD, both symptomatic and asymptomatic, who had rest/regadenoson-stress ⁸²Rb PET/CT data acquisition and arteriography at St. Francis Hospital, studied from January, 2010 through December, 2016. Mean time difference between PET and angiography was 138 ± 388 days. There were no cardiac events (e.g., PCI or MI) between PET and angiography. Patients with unstable ischemic syndromes are routinely excluded from stress perfusion imaging in the laboratory. Patient characteristics are provided in Table 1.

The Institutional Review Board approved this retrospective study and the requirement to obtain informed consent was waived. All data were handled in compliance with the Health Insurance Portability and Accountability Act of 1996.

Angiography. Quantitative coronary angiography was performed at Boston Clinical Research Institute (BCRI, Boston, MA) with PlusPlus software (Sanders Data Systems, Palo Alto, CA). The quantitative reader identified and assessed any lesions with visual stenosis > 20%. Lesions in vessels < 2.0 mm in diameter were not assessed unless the lesion was in a vascular segment that was the primary conduit of circulation for any myocardial wall/segment, or if the artery segments would be ≥ 2.0 mm in diameter if fully perfused. Segment locations for lesions meeting these criteria were recorded and software was used to calculate minimum lumen diameter, mean lesion diameter, lesion length, and percent stenosis. The quantitative reader also assessed TIMI Flow Grade, TIMI Frame Count, TIMI Myocardial Perfusion Grade, and collateral classification on a Rentrop grading system for each of the three major coronary arteries when evaluable images were available.¹⁶

The lesion extent and likelihood of stenosis resulting in a myocardial perfusion defect were scored on a 4-point scale.

Table 1. Patient characteristics tabulated by number of vessel with stenoses $\geq 70\%$

Parameter	No vessels (N = 58)	Any CAD (N = 47)	1-vessel (N = 32)	2-vessel (N = 8)	3-vessel (N = 7)
Age	69 ± 13	69 ± 13	70 ± 12	69 ± 12	72 ± 17
Sex (% male)	59%	62%	62%	50%	71%
BMI (kg·m ⁻²)	31.5 ± 7.7	30.3 ± 8.4	30.8 ± 9.1	32.3 ± 6.4	24.6 ± 3.3
Hx CHF (%)	13%	11%	10%	14%	17%
Hx MI (%)	22%	39%	33%	60%	40%
Hx PCI (%)	39%	36%	39%	40%	20%
Hx CABG (%)	24%	18%	17%	20%	20%
TID	1.09 ± 0.18	1.10 ± 0.18	1.13 ± 0.18	1.05 ± 0.12	1.07 ± 0.12
SSS	6.4 ± 9.5	14.0 ± 11.2*	15.1 ± 12.3*	10.9 ± 7.3	12.6 ± 9.9
SRS	4.0 ± 6.3	6.8 ± 7.2*	7.3 ± 7.5	3.3 ± 3.2	9.0 ± 8.5
SDS	2.4 ± 4.4	7.1 ± 7.4*	7.8 ± 8.2*	7.6 ± 5.8	3.6 ± 2.8
Stress MBF	2.01 ± 1.25	1.50 ± 0.89*	1.63 ± 0.87	1.39 ± 1.06	1.01 ± 0.64
Rest MBF	0.91 ± 0.72	0.82 ± 0.40	0.87 ± 0.44	0.68 ± 0.17	0.77 ± 0.41
MFR	2.41 ± 1.11	1.93 ± 1.02*	2.02 ± 0.96	2.07 ± 1.49	1.34 ± 0.41*
Stress EF (%)	57 ± 19%	47 ± 19%*	54 ± 15%	41 ± 23%	24 ± 14%*†
Rest EF (%)	55 ± 19%	47 ± 19%*	52 ± 16%	44 ± 16%	25 ± 20%*†
ΔEF (%)	2.0 ± 7.8%	0.9 ± 9.3%	2.6 ± 9.5%	- 3.5 ± 8.1%	- 1.9 ± 8.1%
Stress SD	36 ± 21°	45 ± 24°*	38 ± 19°	53 ± 27°*	68 ± 29°*†
Rest SD	36 ± 20°	42 ± 20°	36 ± 16°	47 ± 23°*	66 ± 11°*†
Asynch	11.7 ± 10.3	20.8 ± 11.1*	17.1 ± 9.0	23.3 ± 11.1*	34.7 ± 8.9*†

CAD, Coronary artery disease; BMI, body mass index; Hx, history; CHF, congestive heart failure; MI, myocardial infarction; PCI, percutaneous coronary intervention; CABG, coronary artery bypass graft; TID, transient ischemic dilation; SSS, summed stress score; SRS, summed rest score; SDS, summed difference score; MBF, myocardial blood flow (in units of ml·g⁻¹·min⁻¹); MFR, myocardial flow reserve; EF, ejection fraction; Δ, change; SD, phase histogram standard deviation; Asynch, asynchrony measure *P < .05 vs no vessels; †P < .05 vs 1-vessel

When multiple lesions were scored in one territory, only the largest stenosis was tabulated for that territory on a spreadsheet. Dichotomous rankings also were generated for quantified arterial territories, with $\geq 70\%$ stenosis considered abnormal. Severe CAD was defined as ≥ 2 territories with stenoses $\geq 70\%$, and was termed multi-vessel disease (MVD).

PET Imaging Procedure

Standard patient preparation procedures were followed in conjunction with pharmacologic stress testing using regadenoson, including duration of fasting, abstention from caffeine, and withholding of cardiac medications.^{4,17} Blood pressure, heart rate, and cardiac rhythm were monitored and recorded throughout data acquisition.

At rest, 0.94-1.22 GBq (35-45 mCi) of ⁸²Rb was infused over 20-30 seconds from a ⁸²Sr-⁸²Rb generator (Bracco Diagnostics, Inc). At peak pharmacologic stress, when hemodynamic steady state was achieved, usually 55-60 seconds after initiation of regadenoson injection, an activity similar to that used for rest imaging was infused for stress data acquisition. As noted in previous studies, about 10 seconds after initiation, the generator commenced infusion, which was complete at approximately 30 seconds.¹⁸ The start-time

following commencement of the list-mode scan was a constant 2 minute delay for each patient.

Two PET/CT systems were used during this study. Prior to 2016, PET/CT studies were performed on a Discovery VCT 64 PET/CT (General Electric), with data acquired in 2D mode. After 2016, studies were performed on a D710 PET/CT 64-slice CT system (General Electric), with data acquired in 3D mode.

Myocardial Perfusion Imaging

All PET data were collected in gated list-mode format. The first-pass portion of data were re-binned into a series of consecutive dynamic data sets for 20 3-sec cinematic frames, 5 12-sec frames, and 7 30-sec frames. The myocardial equilibrium portion of data were re-binned as gated data sets for 8 cinematic frames/R-R interval, beginning two minutes after injection until the end of data acquisition at seven minutes.

CT scan transmission data were used to correct for attenuation using the manufacturer's iterative reconstruction software, which also corrected for scatter and random events and normalized for detector inhomogeneities. Data were reconstructed by OSEM (20 subsets; 2 iterations; z-axis filter = "standard"; post-filter = 2.57 mm FWHM).

Semi-automated Emory Cardiac Toolbox v4 software was used to compute MBF.¹⁹ A 1-tissue compartment, one rate constant (microsphere analog) model with spillover effects was used to describe tracer uptake in myocardial tissue. Algorithms automatically identified blood pool and myocardial tissue voxels. Curves sampled at blood pool locations were corrected for myocardial activity “spill over” caused by left ventricle (LV) contraction, respiration, and imperfect spatial resolution. Myocardial tissue curves also were corrected for spill over from the LV blood. Count recovery coefficients (0.8 for tissue; 0.95 for blood) to correct the finite scanner spatial resolution were determined from simulations and were fixed during the fitting. The spillover coefficients were free parameters during the fitting procedure. Spillover from tissue to blood was determined by fitting the global average tissue uptake with three parameters (k_1 and two spillover constants). The corrected blood curve from this fitting was used to determine k_1 and spillover from blood to tissue for each of the 17 segments. After fitting, the blood to tissue rate constants ($k_1 = \text{flow} \times \text{extraction}$) were corrected for flow-dependent extraction using the Renkin and Crone relation with a permeability-surface area product of 2.4.^{20,21}

Rest and stress MBF were calculated for 17 standard LV segments.²² Because the algorithm used to compute resting MBF did not correct for rate-pressure product, and because there is lack of agreement on the precise correction that should be used, we did not correct MBF for the rate-pressure product, consistent with prior ⁸²Rb PET publications.²³ MFR was computed for each segment as stress-MBF/rest-MBF. Global MBF and MFR values were computed as the mean of segmental values 4-17 (Figure 1). Basal-septal segments (numbers 1-3) were excluded from analysis to avoid underestimating MBF due to the LV outflow tract (Figure 2).²⁴ MBFs were generated for left anterior descending (LAD), left circumflex (LCX), and right coronary artery (RCA) territories.

Emory Cardiac Toolbox algorithms also generated a transient ischemic dilatation index (TID), and relative perfusion measurements, including summed stress scores (SSS), summed rest scores (SRS), and summed difference scores (SDS) by applying ⁸²Rb-specific normal limits to perfusion polar maps. Relative perfusion measurements were computed for LV arterial territories and globally. Functional parameters were obtained from gated equilibrium ⁸²Rb PET data. LV end-diastolic and end-systolic volumes were computed, from which ejection fractions (EF) were obtained.²⁵

Systolic and Diastolic Ventricular Asynchrony

Wall thickening was computed at each voxel as % count change from diastole to systole of ⁸²Rb myocardial perfusion polar map counts.²⁶ Each voxel's systolic phase was computed as the onset of mechanical contraction, defined as the phase shift of a 1st-harmonic Fourier fit to counts vs R-wave.²⁷ Diastolic phase was computed as onset of mechanical

relaxation, defined as end crossing point of a 3rd-harmonic Fourier fit to counts vs R-wave.²⁸ The algorithms produced rest and stress phase histograms, phase standard deviation (SD), systolic contraction, and diastolic filling phase polar maps.^{27,28}

Whereas phase SD is a global parameter representing phase dispersion, we also wished to assess the capability of phase analysis to identify individual stenosed territories. Accordingly, a medical imaging physicist, without knowledge of angiographic or other clinical information, scored regional asynchrony within each coronary territory on a 5-point scale while viewing simultaneously displayed anonymized systolic and diastolic rest and stress phase histograms, phase polar maps, and perfusion polar maps. Scores were assigned to each territory for rest systole, rest diastole, stress systole, and stress diastole polar phase maps. The lowest score (0 = “normal”) was assigned to a territory if rest and stress systolic phase histograms were narrow peaks centered near 1/3 R-R, and diastolic phase histograms were narrow peaks centered near 2/3 R-R, along with rest and stress phase maps displaying uniform contraction throughout that territory. The highest score (4 = “markedly asynchronous extensive territory”) was assigned to a territory if phase histograms were broad or scattered and corresponded to a large % of contractions occurring out of phase for a large % of pixels of that territory (Figure 3). Intermediate scores from 1-3 were assigned for varying degrees of territorial asynchrony between those two extremes. A single composite value of visual regional phase asynchrony (Asynch) was formed, generated as the sum of all systolic and diastolic rest and stress visual territorial scores, for which the highest possible global value was 48. The lowest possible Asynch global score was “0” for a normal subject (Figure 4).

On a separate occasion, the same observer rescored all anonymized phase histograms and maps to generate independent Asynch scores, without reference to previous scores or clinical information, to enable determination of Asynch intra-observer reproducibility. For a random subgroup of 50 patients, a nuclear cardiologist independently scored all anonymized phase maps and generated Asynch scores without knowledge of the first observer's scores or clinical information, to enable determination of Asynch inter-observer agreement.

Statistical Analysis

Analyses were performed using commercially available software (“MedCalc” Statistical Software version 18; MedCalc Software bvba, Ostend, Belgium). Values are reported as means \pm one standard deviation. Continuous variables were assessed by the χ^2 test to determine normality of distribution. The unpaired or paired t test, as appropriate, compared values between groups for continuous variables that were normally distributed; otherwise, the Mann-Whitney or Wilcoxon test was used. χ^2 analysis of proportions compared ratios. For each test parameter, the “Medcalc” software reported the value of the receiver operating characteristics area under curve (ROC AUC) that was obtained by determining the threshold criterion

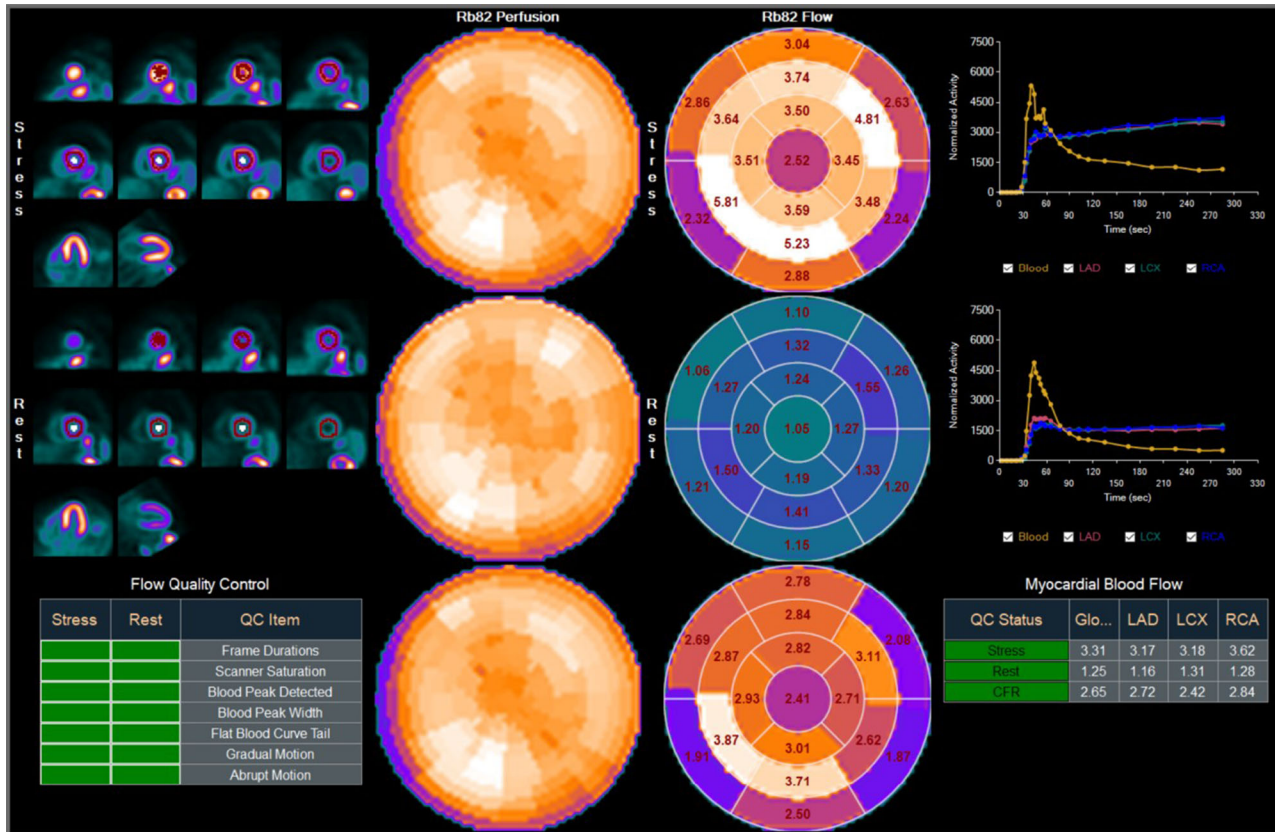


Figure 1. Quality control screen of MBF for a patient without CAD.

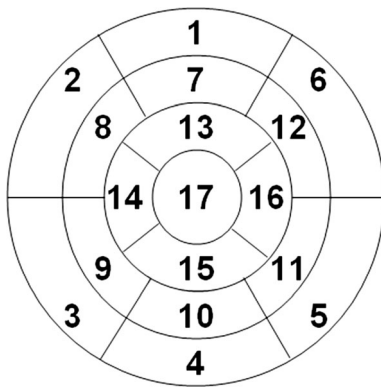


Figure 2. ACC/AHA 17-segment map.

value that optimized the Youden index; the threshold value subsequently was used to obtain dichotomous accuracy, sensitivity, specificity, positive predictive value (PPV), and negative predictive value (NPV). Significance of difference of ROC AUC results was assessed.²⁹ χ^2 rank correlation with Spearman's ρ quantified trends of variables with increasing numbers of stenosed vessels among patients. Intra-observer reproducibility and inter-observer agreement were assessed by Bland-Altman analysis. For all tests, probability (P) < .05 was defined as statistically significant.

RESULTS

Parameters in Patients With and Without Obstructive CAD

Among the 105 patients 58 had native vessels or bypass conduits with no obstructive CAD. Among the 47 patients who had at least one coronary territory with significant CAD, 32 had single-vessel CAD and 15 had multi-vessel CAD, of whom 7 had triple-vessel CAD. There were no differences in age, gender, or body mass index between groups (Table 1). Patients with no current obstructive CAD had a similar frequency of history of CHF, MI, CABG, and PCI as those with CAD. Hemodynamic response to regadenoson was similar in all patient subgroups, with an increase in heart rate of 22 ± 13 bpm.

Patients without obstructive CAD had a resting MBF of 0.91 ± 0.72 mL·g⁻¹·min⁻¹, stress MBF of 2.01 ± 1.25 mL·g⁻¹·min⁻¹ and MFR of 2.41 ± 1.11 . Patients with any CAD had similar resting MBF of 0.82 ± 0.40 mL·g⁻¹·min⁻¹, but lower stress MBF of 1.50 ± 0.89 mL·g⁻¹·min⁻¹ ($P = .01$), and lower MFR of 1.93 ± 1.02 ($P = .02$) (Table 1). In addition, relative perfusion scores, rest and stress EF, and Asynch

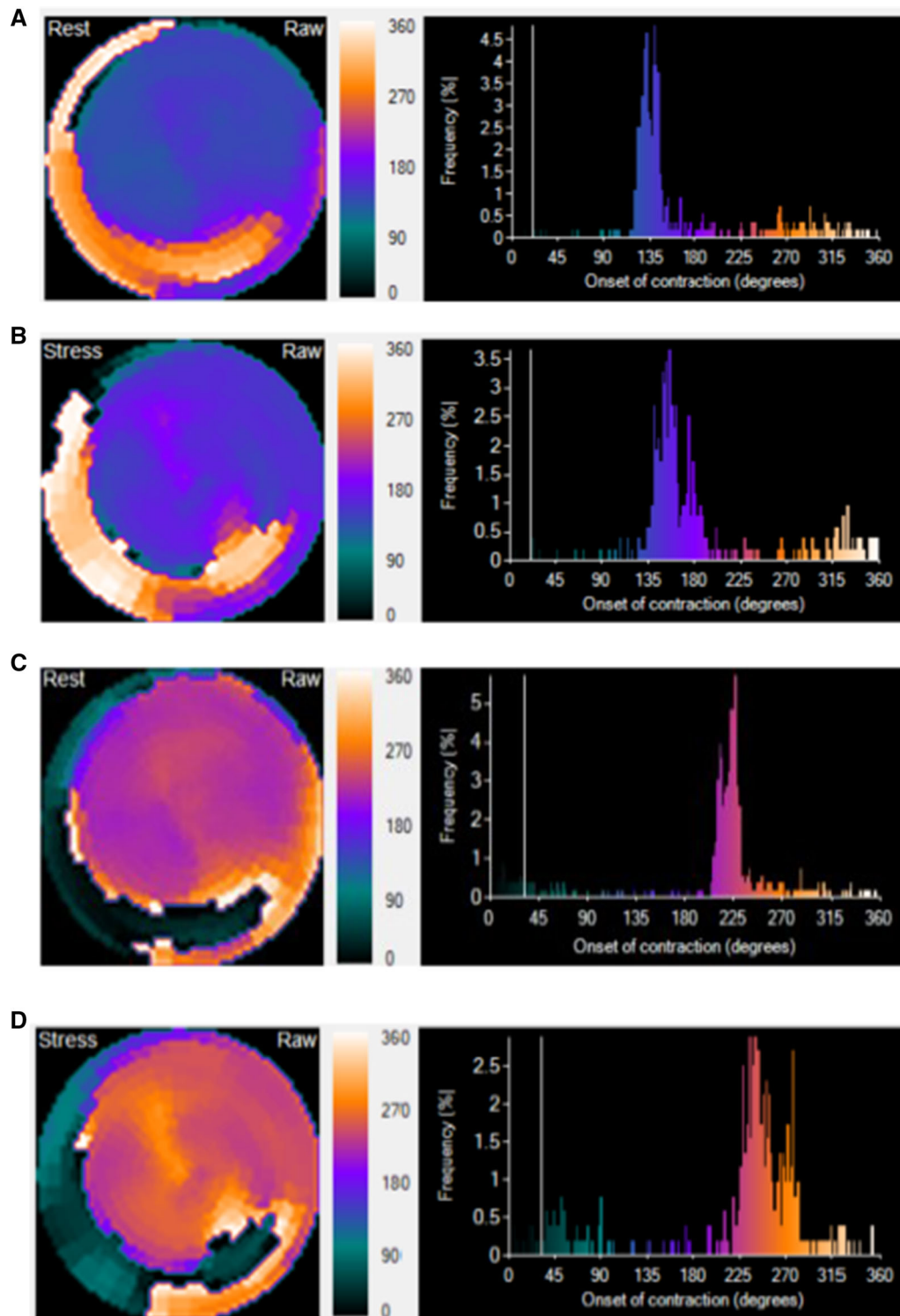


Figure 3. For a patient with LAD and RCA stenoses, LAD, LCX and RCA territories of the phase maps were scored 3,0,3 for rest systole (A), 4,0,4 for stress systole (B), 3,0,3 for rest diastole (C), and 4,0,4 for stress diastole (D), respectively, for a total “Asynch” value of 28.

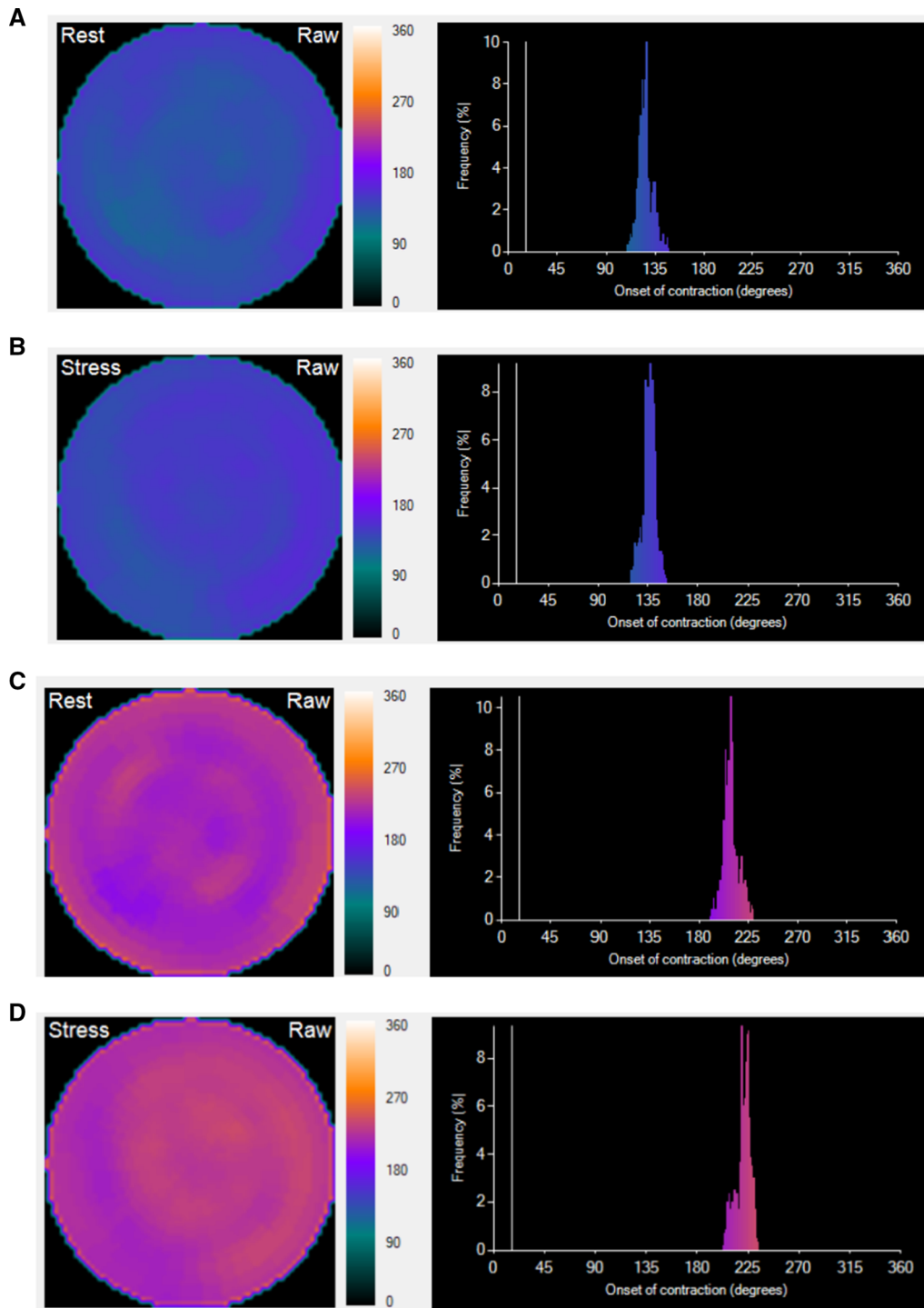


Figure 4. For the same patient without CAD of Figure 1, systolic phase maps and histograms at rest (A) and stress (B), and diastolic phase maps and histograms at rest (C) and stress (D). All 3 arterial territories of all 4 phase maps were scored 0, for a total “Asynch” value of 0.

measures differed between patients with and without any CAD. Among all parameters, the Asynch score had highest ROC AUC ($74 \pm 5\%$) for diagnosing any CAD, with sensitivity = 62% and specificity = 77%. By

Bland-Altman analysis, Asynch intra-observer differences were uncorrelated with means ($r = 0.09$, $P = .35$), with no trend ($P = .18$), and small bias (1.0 ± 0.3 , $P = .002$), but with wide ± 1.96 standard

deviation limits of agreement of -8.6 to $+7.2$. There was no statistically significant trend ($P = .26$) or bias ($P = .26$) for inter-observer agreement, and differences were not correlated with means ($r = 0.16$, $P = .26$), but limits of agreement of -9.5 to $+5.0$ were wide.

There were 250 vessels with no stenoses or with stenoses $< 70\%$, and 65 vessels had stenoses $\geq 70\%$, distributed as 22 LAD, 18 LCX, and 25 RCA territories. Resting MBF was similar regardless of the number of arteries involved per patient, but stress MBF decreased progressively with increasing numbers of involved arteries (Table 1). Other descriptors that trended significantly with increasing involvement with CAD included relative perfusion scores; strongest rank correlations were for Asynch ($\rho = +0.47$, $P < .0001$) and stress EF ($\rho = -0.35$, $P = .0003$).

Identifying Patients with Multi-vessel Coronary Disease

Parameters that significantly distinguished patients with multi-vessel disease from those with no obstructive CAD or one vessel disease included stress MBF, stress EF, and Asynch score (Table 2). Relative perfusion scores were less helpful, with ROC AUC of only 51-63%, significantly less than the 84% ROC AUC of the Asynch score ($P < .0001$). Stress EF was comparable to Asynch in identifying patients with MVD (ROC AUC $80 \pm 7\%$ vs $84 \pm 6\%$, $P = .96$).

Patients with triple-vessel CAD had lowest stress MBF ($1.01 \pm 0.64 \text{ mL}\cdot\text{g}^{-1}\cdot\text{min}^{-1}$) and lowest MFR (1.34 ± 0.41) in the patient cohort (Table 1). Absolute perfusion measurements were effective at discriminating patients with triple-vessel disease (MFR ROC AUC 81%). The strongest associations were found for Asynch (ROC AUC 92%); relative perfusion measures were not effective in discriminating triple-vessel CAD (ROC AUC 53-59%) (Table 3). All tested parameters were highly effective at ruling out MVD and triple-vessels disease, with NPV values of 95-100% for triple-vessels disease (Table 3).

Individual Coronary Arteries

Stress MBF and MFR had accuracy of $70 \pm 4\%$ and $72 \pm 4\%$ for isolating individual stenosed arterial territories, with significantly different MFR (1.72 ± 1.07 vs 2.32 ± 1.12 , $P < .0001$) for vessels with $< 70\%$ stenosis compared to those with $\geq 70\%$ stenosis (Table 4). The accuracy of MFR for identifying LAD, LCX and RCA stenosed territories was similar (ROC AUC = $73 \pm 6\%$, $76 \pm 6\%$, and $69 \pm 7\%$, respectively).

The most accurate parameter identifying individual stenosed vessels was Asynch (ROC AUC = 81%)

(Table 4), for which ROC AUC values for LAD, LCX and RCA territories were similar ($79 \pm 5\%$, $82 \pm 5\%$, and $81 \pm 5\%$, respectively). Asynch also had the highest negative predictive value of all parameters (92%), which is efficacious in ruling out CAD for individual territories (Table 4).

DISCUSSION

With the advent of ⁸²Sr-⁸²Rb generators, the potential for routinely measuring ⁸²Rb-PET MBF has become feasible. Algorithms for calculating MBF using ⁸²Rb were proposed and validated,⁴ and investigations suggested that MBF and MFR determination had a significant role to play in clinical practice. Absolute flow measurements added accuracy in distinguishing patients with and without CAD, could exclude the possibility of patients having severe triple-vessel CAD, and added significant value in predicting short term cardiac events.¹⁰ There have been multiple algorithms developed that currently are used to measure MBF and MFR using PET MPI.³⁰ In a comparison of three of these algorithms in normal subjects, there was general agreement that average MFR for women was 2.7 and for men, 2.5.³¹ However, there was significant variation among algorithms,³² and a considerable proportion of these “normal” patients had MFR below 2.0.

Studies that have attempted to use MFR to aid in diagnosing CAD have had variable results. Fiechter et al performed PET MPI with quantified MBF using ¹³NH₃ in 73 clinical patients with suspected CAD undergoing conventional angiography.³³ They found that adding MFR < 2.0 to conventional imaging criteria allowed them to increase sensitivity for CAD to 96%, with a specificity of 80%. Naya et al studied 290 patients with suspected CAD undergoing conventional angiography, excluding those with history of MI and revascularization.³⁴ They found a similar threshold of MFR < 1.93 maximized their ability to detect high risk coronary anatomy with high sensitivity (89%), but low specificity (36%). The authors concluded that MFR was a helpful adjunct to identify or help exclude high risk coronary disease, but could not be used to distinguish between decreased flows due to epicardial stenosis vs microvascular CAD.

In our study the goal was to determine the general clinical utility of MBF determinations in characterizing CAD in a heterogeneous group of patients presenting to a nuclear cardiology PET laboratory. Consequently, our patient group consisted of individuals with no CAD, established CAD with MI, PCI, and CABG, and who had a wide range of LV function, averaging 55% for patients with minimal CAD to 25% in patients with extensive CAD. To minimize qualitative variability of

Table 2. Test performance results for parameters identifying patients with multi-vessel disease.

Parameter	ROC threshold	ROC AUC (%)	Dichotomous accuracy (%)	Sensitivity (%)	Specificity (%)	PPV (%)	NPV (%)	Mean CAD+	Mean CAD-
TID	< 1.21	56 ± 7*	33*	93	23*	17*	95	1.06 ± 0.12	1.10 ± 0.18
SSS	> 8	57 ± 8*	63*	71	61*	24*	93	10.4 ± 7.8	9.3 ± 10.0
SRS	> 3	51 ± 8*	61*	57	61*	20*	90	5.7 ± 6.1	5.1 ± 6.7
SDS	> 3	63 ± 8*	65*	71	64*	24*	92	4.6 ± 5.1	4.2 ± 6.7
Stress MIBF	< 0.94	75 ± 8	83	60	87	43	93	1.21 ± 0.88†	1.88 ± 1.14
Rest MIBF	< 0.85	59 ± 7*	49	80	43*	19*	93	0.72 ± 0.30†	0.90 ± 0.64
MFR	< 1.76	73 ± 7*	66	80	64*	27	95	1.72 ± 1.15†	2.27 ± 1.08
Stress EF	< 24%	80 ± 7	88	60	93	60	93	36 ± 20%†	54 ± 18%
Rest EF	< 41%	75 ± 7	76	67	78*	33	93	25 ± 20%†	55 ± 18%
ΔEF	< - 4%	66 ± 8*	75	53	79*	30	91	- 3 ± 8%†	+ 2 ± 8%
Stress SD	> 58°	74 ± 8	84	67	87	43	94	60 ± 29°†	37 ± 20°
Rest SD	> 53°	76 ± 8	77	73	79*	35	95	56 ± 20°†	36 ± 18°
Asynch	> 26	84 ± 6	87	67	90	50	94	29 ± 11†	14 ± 10%

ROC AUC, Receiver operating characteristics area under curve; PPV, positive predictive value; NPV, negative predictive value; CAD+, patients with coronary artery disease; CAD-, patients who did not have coronary artery disease

* P < .05 statistically different from Asynch results; † P < .05 for CAD+ vs CAD-

Table 3. Test performance results for parameters identifying patients with triple-vessel disease.

Parameter	ROC threshold	ROC AUC (%)	Dichotomous accuracy (%)	Sensitivity (%)	Specificity (%)	PPV (%)	NPV (%)	Mean CAD+	Mean CAD-
TID	< 1.21	53 ± 11*	27*	100	22*	8*	100	1.76 ± 0.12	1.10 ± 0.18
SSS	> 10	55 ± 14*	64*	67	63*	12	97	10.5 ± 9.0	9.4 ± 8.0
SRS	> 3	59 ± 14	60*	71	60*	11*	97	6.8 ± 6.9	5.1 ± 6.6
SDS	> 3	53 ± 11*	61*	57	61*	10*	95	3.7 ± 3.0	4.3 ± 6.7
Stress MBF	< 1.08	80 ± 10	77*	86	76*	21	99	1.84 ± 1.14 [†]	1.01 ± 0.64
Rest MBF	< 0.63	58 ± 13*	68	71	67*	14	97	0.77 ± 0.41	0.88 ± 0.61
MFR	< 1.71	81 ± 6	69	100	63*	18	100	1.34 ± 0.41 [†]	2.26 ± 1.11
Stress EF	< 35%	91 ± 5	83	86	83	26	99	24 ± 14% [†]	57 ± 18%
Rest EF	< 19%	87 ± 10	96*	71	98*	71	98	25 ± 20% [†]	55 ± 18%
ΔEF	< + 3%	61 ± 11*	43*	86	40*	9*	98	- 1 ± 8%	+ 3 ± 8%
Stress SD	> 79°	79 ± 11	91	71	93	42	98	68 ± 29° [†]	38 ± 21°
Rest SD	> 53°	89 ± 4	77*	100	77*	23	100	66 ± 11° [†]	37 ± 19°
Asynch	> 28	92 ± 6	88	86	89	33	99	34 ± 9 [†]	14 ± 10

* *P* < .05 statistically different from Asynch results; [†] *P* < .05 for CAD+ vs CAD-

Table 4. Test performance results for parameters identifying individual arterial territories with stenosis $\geq 70\%$.

Parameter	ROC threshold	ROC AUC (%)	Dichotomous accuracy (%)	Sensitivity (%)	Specificity (%)	PPV (%)	NPV (%)	Mean CAD+	Mean CAD-
SSS	> 6	66 ± 4*	77	46*	85*	44	86*	6.2 ± 5.9 [†]	2.8 ± 4.0
SRS	> 3	60 ± 4*	73	40*	82*	35	84*	3.0 ± 3.6 [†]	1.6 ± 2.5
SDS	> 1	66 ± 4*	72	54*	76	37	86*	3.3 ± 4.1 [†]	1.2 ± 2.5
Stress MIBF	< 1.07	70 ± 4*	73	60	76	39	88	1.25 ± 0.79 [†]	1.88 ± 1.20
Rest MIBF	< 0.63	54 ± 4*	62*	46*	66	26	82*	0.78 ± 0.38	0.89 ± 0.64
MFR	< 1.88	72 ± 4*	63*	79	59*	33	91	1.72 ± 1.07 [†]	2.32 ± 1.12
Asynch	> 6	81 ± 3	74	75	74	42	92	9.5 ± 4.3 [†]	4.1 ± 4.2

* $P < .05$ statistically different from Asynch results; [†] $P < .05$ for CAD+ vs CAD-

angiogram interpretation,¹⁵ all cineangiograms were assessed by quantitative methodology at BCRI.

Our MBF and MFR values are consistent with values reported by other investigators. Despite a significant percentage of patients with a history of MI on presentation, resting MBF values averaged 0.82 mL·g⁻¹·min⁻¹, similar to those of Efseaff et al (0.79-0.88 mL·g⁻¹·min⁻¹).³⁵ MFR in patients who did not have angiographic evidence of obstructive CAD > 70% was 2.41 ± 1.11, similar to values cited by other authors as indicative of a low probability of CAD.³⁶ MFR decreased progressively with increasing CAD to 1.34 ± 0.41 in patients with triple-vessel coronary disease, comparable to MFR of 1.3 obtained by Ziadi et al in a study of 120 patients with CAD who underwent qualitative angiography.³⁷

MFR was somewhat effective for discriminating patients with multi-vessel CAD from those with single-vessel disease or no CAD, and achieved a sensitivity of 80% and specificity of 64% using a threshold of 1.76. In the study by Ziadi et al,³⁶ a value of just above 1.5 represented the inflection point of a plot of triple-vessel disease vs MFR. Our 100% sensitivity of MFR for triple-vessel CAD is higher than our 80% sensitivity for multi-vessel CAD. However, in both cases, MFR was superior to relative perfusion scores for identifying CAD, while other imaging parameters were also significant predictors, including stress EF. In our study, we also measured LV asynchrony. We found that parameter with the highest ROC AUC for detecting multi-vessel CAD was Asynch (84%).

As reported in other studies,³³ in our study relative perfusion scores were less effective than measurement of MFR. Compared to the accuracy of 80% cited by Muzik et al using ¹³NH₃ MFR to detect individual coronary artery stenosis,⁸ our ROC AUC of 72% was lower using ⁸²Rb MFR, but was similar using regional asynchrony (ROC AUC = 81%).

One goal of performing MFR determinations with PET is to identify a threshold that reliably separates patients with and without significant obstructive epicardial coronary disease. MFR values of 2.0-2.5 have been the ranges frequently cited for “normal.”³⁶ However, reviews of the physiology of coronary anatomy indicate that this is a complex issue.³⁸ MFR may be below thresholds due to elevated resting MBF induced by hypertension, downstream microvascular disease in the absence of epicardial coronary stenosis, or due to variance imposed by age, gender, isotope, or quantitative algorithm. Bateman et al, pointed out that in a study by Sunderland et al of 49 patients with low probability of CAD, 17% had MFR less than the accepted threshold of 2.0, suggesting that the range of normal may be broader than proposed.^{31,32} Our cohort, containing

patients with MI and revascularization, was substantially different than Sunderland's low probability patients, and was similar to that of Johnson and Gould et al,³⁹ encompassing the full clinical range of patients presenting with CAD. Despite differences in patient populations, MFR variability seen in our patients without obstructive coronary lesions paralleled that seen by Sunderland. These data reinforce the concept that it remains difficult to consider a simple threshold value of MFR as uniquely separating patients with and without obstructive coronary lesions.

Our study also illustrated the potential of LV asynchrony measurements as an important adjunct for identifying individual coronary artery stenoses. Previously it has been demonstrated that mechanical asynchrony is related to global LV MFR.⁴⁰ Asynchrony determinations from ⁸²Rb PET myocardial perfusion imaging generally use expressions of global, not regional, phase bandwidth, and standard deviation.²⁶ Statistical noise has been an obstacle for using LV asynchrony to identify segmental coronary stenoses. In the current study, we formulated a simple qualitative scale that could be applied to regional asynchrony, which had an acceptable degree of intra- and inter-observer reproducibility. Our results suggest that the regional asynchrony scale is effective in noninvasively assessing individual coronary arteries. Whether this construct might be synergistic with MFR could not be established from the limited number of patients in the current study.

NEW KNOWLEDGE GAINED

MFR as a single descriptor was limited in its sensitivity and accuracy for defining jeopardized myocardium. Regional asynchrony agreed more strongly with quantitative coronary angiography than regional MFR.

LIMITATIONS

A limitation of our study is that data were derived from a single center. Though patients were unselected, in that they comprised a wide spectrum of coronary diagnoses, the study group did represent only a sub-population of all patients, since they were required to have both cardiac PET and coronary angiograms, suitable for quantitation. These requirements resulted in a cohort with a high prevalence of CAD. Thus, even our patients scored as free of serious $\geq 70\%$ coronary lesions most likely had some degree of non-obstructive CAD and microvascular disease.

Since PET MBF is a physiologic descriptor, and angiography is usually anatomic, there is difficulty in selecting the correct catheterization parameter to use as

a gold standard. Fractional flow reserve is more closely related to MBF, but also may give disparate results from PET MFR due to multiple stenosis, and lack of accountability for microvascular disease.^{41,42} We chose to contrast PET MFR with quantitative angiographic parameters because of their general acceptance and availability. We recognize that further studies are necessary to relate PET MFR to physiologic catheterization parameters.

There are numerous approaches to quantifying absolute MBF from first-pass PET data, with each using its own unique modeling assumptions.³⁰ It is possible that applying other algorithms to our data would have resulted in obtaining somewhat different MFR thresholds for defining single and multi-vessel CAD. However, as described above, the results we obtained using the specific algorithms we employed appear to have yielded MFR findings consistent with those of previous investigators.³³⁻³⁶

Our data suggest that visual regional asynchrony assessment was an effective means of identifying individual stenosed arteries and is a promising approach to isolating diseased vessels. Nevertheless, this is a subjective measure with wide limits of agreement. Efforts toward automating the quantification of regional asynchrony, such as adding regional phase SD measurement to global phase SD, may be worthwhile, and should be investigated in a larger cohort of patients.

CONCLUSIONS

⁸²Rb PET/CT function and perfusion measurements accurately identify patients with MVD and individual stenosed territories, with visual regional phase asynchrony measurements corresponding significantly to patients with CAD.

Disclosures

This investigation was supported in part by grants from Astellas Pharma Global Development Inc. to St. Francis Hospital and R01HL094438 and R44HL123069 to Emory University. John R. Votaw, C. David Cooke and Kenneth J. Nichols participate in royalties from Syntermed, Inc. We wish to thank J.J. Mathew for his expert assistance in data acquisition and processing of the PET/CT data, and M. Cochet and C. Popma, for their processing of the angiography data at BCRI.

References

1. Bateman TM, Heller GV, McGhie AI, Friedman JD, Case JA, Bryngelson JR, et al. Diagnostic accuracy of rest/stress ECG-gated Rb-82 myocardial PET: Comparison with ECG-gated Tc-99 m sestamibi SPECT. *J Nucl Cardiol* 2006;13:24-33.

- McArdle BA, Dowsley TF, DeKemp RA, Wells GA, Beanlands RS. Does rubidium-82 PET have superior accuracy to SPECT perfusion imaging for the diagnosis of obstructive coronary disease? *J Am Coll Cardiol* 2012;60:1828-37.
- Bateman TM, Dilsizian V, Beanlands RS, DePuey G, Heller GV, Wolinsky DA. American Society of Nuclear Cardiology and Society of Nuclear Medicine and Molecular Imaging. Joint Position Statement on the Clinical Indications for Myocardial Perfusion PET. *J Nucl Cardiol* 2016. <https://doi.org/10.1007/s12350-016-0626-9>.
- Gould KL. Clinical cardiac PET using generator-produced Rb-82: A review. *Cardiovasc Interv Radiol* 1989;12:245-51.
- DeKemp RA, Declerck J, Klein R, Pan X-B, Nakazato R, Tonge C, et al. Multisoftware reproducibility study of stress and rest myocardial blood flow assessed with 3D dynamic PET/CT and a 1-tissue-compartment model of ⁸²Rb kinetics. *J Nucl Med* 2013;54:571-7.
- Lautamaki R, George RT, Kitagawa K, Higuchi T, Merrill J, Voicu C, et al. Rubidium-82 PET-CT for quantitative assessment of myocardial blood flow: Validation in a canine model of coronary artery stenosis. *Eur J Nucl Med Mol Imaging* 2009;36:576-86.
- Duvernoy CS, vom Dahl J, Laubenbacher C, Schwaiger M. The role of nitrogen 13 ammonia positron emission tomography in predicting functional outcome after coronary revascularization. *J Nucl Cardiol* 1995;2:499-506.
- Muzik O, Duvernoy C, Beanlands RS, Sawada S, Dayanikli F, Wolfe ER, et al. Assessment of diagnostic performance of quantitative flow measurements in normal subjects and patients with angiographically documented coronary artery disease by means of nitrogen-13 ammonia and positron emission tomography. *J Am Coll Cardiol* 1998;31:534-40.
- Herzog BA, Husmann L, Valenta I, Gaemperli O, Siegrist PT, Tay FM, et al. Long-term prognostic value of 13 N-ammonia myocardial perfusion positron emission tomography added value of coronary flow reserve. *J Am Coll Cardiol* 2009;54:150-6.
- Fukushima K, Javadi MS, Higuschi T, Lautamaki R, Merrill J, Nekolla SG, et al. Prediction of short-term cardiovascular events using quantification of global myocardial flow reserve in patients referred for clinical ⁸²Rb PET perfusion imaging. *J Nucl Med* 2011;52:726-32.
- Murthy VL, Bateman TM, Beanlands RS, Berman DS, Borges-Neto S, Chareonthaitawee P, et al. Clinical quantification of myocardial blood flow using PET: Joint position paper of the SNMMI Cardiovascular Council and the ASNC. *J Nucl Cardiol* 2018;25:269-97.
- CPT 0482T; <http://www.codingahead.com/2017/11/2018-new-cpt-codes.html>.
- Hajjiri MM, Leavitt MB, Zheng H, Spooner AE, Fischman AJ, Gewirtz H. Comparison of positron emission tomography measurement of adenosine-stimulated absolute myocardial blood flow versus relative myocardial tracer content for physiological assessment of coronary artery stenosis severity and location. *JACC Cardiovasc Imaging* 2009;2:751-8.
- Johnson NP, Gould KL. Integrating noninvasive absolute flow, coronary flow reserve, and ischemic thresholds into a comprehensive map of physiological severity. *JACC Cardiovasc Imaging* 2012;5:430-40.
- Motwani M, Motlagh M, Gupta A, Berman DS, Slomka PJ. Reasons and implications of agreements and disagreements between coronary flow reserve, fractional flow reserve, and myocardial perfusion imaging. *J Nucl Cardiol* 2018;25:104-19.
- Rentrop KP, Cohen M, Blanke H, Phillips RA. Changes in collateral channel filling immediately after controlled coronary artery occlusion by an angioplasty balloon in human subjects. *J Am Coll Cardiol* 1985;5:587-92.
- Bravo PE, Pozios I, Pinheiro A, Merrill J, Tsui BMW, Wahl RL, et al. Comparison and effectiveness of regadenoson versus dipyridamole on stress electrocardiographic changes during positron emission tomography evaluation of patients with hypertrophic cardiomyopathy. *Am J Cardiol* 2012;110:1033-9.
- Johnson NP, Gould KL. Regadenoson versus dipyridamole hyperemia for cardiac PET imaging. *JACC Cardiovasc Imaging* 2015;8:438-47.
- Votaw JR, Packard RRS. Technical aspects of acquiring and measuring myocardial blood flow: Method, technique, and QA. *J Nucl Cardiol* 2017. <https://doi.org/10.1007/s12350-017-1049-y>.
- Renkin EM. Transport of potassium-42 from blood to tissue isolated mammalian skeletal muscles. *Am J Physiol* 1959;197:1205-10.
- Crone C. Permeability of capillaries in various organs as determined by use of the indicator diffusion method. *Acta Physiol Scand* 1963;58:292-305.
- Cerqueira MD, Weissman NJ, Dilsizian V, Jacobs AK, Kaul S, Laskey WK, et al. Standardized myocardial segmentation and nomenclature for tomographic imaging of the heart: A statement for healthcare professionals from the Cardiac Imaging Committee of the Council on Clinical Cardiology of the American Heart Association. *Circulation* 2002;105:539-42.
- Ziadi MC, deKemp RA, Williams KA, Guo A, Chow BJW, Renaud JM, et al. Impaired myocardial flow reserve on Rubidium-82 positron emission tomography imaging predicts adverse outcomes in patients assessed for myocardial ischemia. *J Am Coll Cardiol* 2011;58:740-8.
- Van Tosh A, Reichek N, Palestro CJ, Nichols KJ. Effect of outflow tract contributions to ⁸²Rb-PET global myocardial blood flow computations. *J Nucl Med Technol* 2016;44:78-84.
- Faber TL, Cooke CD, Folks RD, Vansant JP, Nichols KJ, DePuey EG, et al. Left ventricular function from gated SPECT perfusion images: An integrated method. *J Nucl Med* 1999;40:650-9.
- Cooke CD, Esteves FP, Chen J, Garcia EV. Left ventricular mechanical synchrony from stress and rest ⁸²Rb PET myocardial perfusion ECG-gated studies: Differentiating normal from LBBB patients. *J Nucl Cardiol* 2011;18:1076-85.
- Chen J, Garcia EV, Folks RD, Cooke CD, Faber TL, Tauxe EL, et al. Onset of left ventricular mechanical contraction as determined by phase analysis of ECG-gated myocardial perfusion SPECT imaging: Development of a diagnostic tool for assessment of cardiac mechanical dyssynchrony. *J Nucl Cardiol* 2005;12:687-95.
- Boogers MJ, Chen J, Veltman CE, van Bommel RJ, Mooyaart EAQ, Al Younis I, et al. Left ventricular diastolic dyssynchrony assessed with phase analysis of gated myocardial perfusion SPECT: A comparison with tissue Doppler imaging. *Eur J Nucl Med Mol Imaging* 2011;38:2031-9.
- DeLong ER, DeLong DM, Clarke-Pearson DL. Comparing the areas under two or more correlated receiver operating characteristic curves: A nonparametric approach. *Biometrics* 1988;44:837-45.
- Murthy VL, Lee BC, Sitek A, Naya M, Moody J, Polavarapu V, et al. Comparison and prognostic validation of multiple methods of quantification of myocardial blood flow with ⁸²Rb PET. *J Nucl Med* 2014;55:1952-8.
- Sunderland JJ, Pan X-B, Declerck J, Menda Y. Dependency of cardiac rubidium-82 imaging quantitative measures on age, gender, vascular territory, and software in a cardiovascular normal population. *J Nucl Cardiol* 2015;22:72-84.

32. Bateman TM, Case JA. Variability in normal myocardial blood flow measurements: Physiologic, methodologic, or protocol related? *J Nucl Cardiol* 2015;22:85-8.
33. Fiechter M, Ghadri JR, Gebhard C, Fuchs TA, Pazhenkottil AP, Nkoulou RN, et al. Diagnostic value of ¹³N-ammonia myocardial perfusion PET: Added value of myocardial flow reserve. *J Nucl Med* 2012;53:1230-4.
34. Naya M, Murthy VL, Taqueti VR, Foster CR, Klein J, Garber M, et al. Preserved coronary flow reserve effectively excludes high-risk coronary artery disease on angiography. *J Nucl Med* 2014;55:248-55.
35. Efseaff M, Klein R, Ziadi MC, Beanlands RS, deKemp RA. Short-term repeatability of resting myocardial blood flow measurements using rubidium-82 PET imaging. *J Nucl Cardiol* 2012;19:997-1006.
36. Ziadi MC, Beanlands RS. The clinical utility of assessing myocardial blood flow using positron emission tomography. *J Nucl Cardiol* 2010;17:571-81.
37. Ziadi MC, deKemp RA, Williams K, Guo A, Renaud JM, Chow BJW, et al. Does quantification of myocardial flow reserve using rubidium-82 positron emission tomography facilitate detection of multivessel coronary artery disease? *J Nucl Cardiol* 2012;19:670-80.
38. Johnson NP, Tóth GG, Lai D, Zhu H, Açar G, Agostoni P, et al. Prognostic value of fractional flow reserve linking physiologic severity to clinical outcomes. *JACC Cardiovasc Imaging* 2014;64:1641-54.
39. Johnson NP, Kirkeeide RL, Gould KL. Is discordance of coronary flow reserve and fractional flow reserve due to methodology or clinically relevant coronary pathophysiology? *JACC Cardiovasc Imaging* 2012;5:193-202.
40. Van Tosh A, Votaw JR, Cooke CD, Reichek N, Palestro CJ, Nichols KJ. Relationships between left ventricular asynchrony and myocardial blood flow. *J Nucl Cardiol* 2017;24:43-52.
41. Gould KL, Johnson NP, Bateman TM, Beanlands RS, Bengel FM, Bober R, et al. Anatomic versus physiologic assessment of coronary artery disease. Role of coronary flow reserve, fractional flow reserve, and positron emission tomography imaging in revascularization decision-making. *J Am Coll Cardiol* 2013;62:1639-53.
42. Johnson NP, Gould KL. Integrating noninvasive absolute flow, coronary flow reserve, and ischemic thresholds into a comprehensive map of physiological severity. *JACC Cardiovasc Imaging* 2012;5:430-40.